Binary Salts of Substituted Pyridines and L-Tartaric Acid as Nonlinear Optical Organic Materials: Crystal Structure of L-Tartaric Acid–4-Dimethylaminopyridine (1:1) Dihydrate Salt

Parthasarathi Dastidar,[a] Tayur N. Guru Row,[a,b] B. R. Prasad,[c] C. K. Subramanian[c] and Santanu Bhattacharya[*,a]
[a] *Department of Organic Chemistry, Indian Institute of Science, Bangalore 560 012, India*
[b] *Solid State and Structural Chemistry Unit, Indian Institute of Science, Bangalore 560 012, India*
[c] *Department of Physics, Indian Institute of Science, Bangalore 560 012, India*

A number of salts of substituted pyridines with L-tartaric acid were prepared. Their nonlinear optical behaviour *e.g.* second harmonic generation (SHG) activity was measured. The crystal structure of L-tartaric acid–4-dimethylaminopyridine (1:1) dihydrate salt **1** was determined in order to understand the relationship between crystal packing and SHG activity within salt **1**.

The search for new materials possessing high nonlinear optical (NLO) activities surpassing the ones already existing has been pursued extensively in recent years[1] due to their wide range of applications in the second and third harmonic generations,[2] optical bistability,[3] phase conjugation,[4] *etc*. Organic NLO materials are in general more versatile compared to their inorganic counterparts due to larger second-order molecular hyperpolarizability (β), higher resistance to optical damage, more favourable physical properties and easier synthetic manipulations. Synthetic efforts have been mainly concentrated on tuning molecular structures so as to achieve larger β values and hence more pronounced NLO effects.[5,6] But molecules having large βs do not necessarily ensure excellent NLO effects, *viz*. second harmonic generation (SHG) in their crystalline state, due to the frequent occurrence of centrosymmetric crystals or unfavourable packing of the molecules in the crystal lattice.[7] Therefore, it would be useful to generate systems which could easily be prepared synthetically. It is also desirable to obtain crystals of adequate quality so that the crystalline features may be studied in detail. This would enable one to understand factors which relate to the packing of individual molecular/ionic dipoles within the lattice.

Table 1 Physical data of the salts

Entry	Base (M.p./°C)	M.p./°C (Salt)	SHG activity *vs*. urea
1	4-Amino[a] (158–159)	103–105	1.090
2	4-Dimethylamino[a] (114–115)	192–195	1.002
3	4-(*p*-Nitrobenzyl)[a] (70–72)	174–176	1.17
4	2,6-Dimethyl[a] (liquid)	60–62	+ve[e]
5	2-Amino-5-chloro[a] (136–137)	158–159	+ve[e]
6	8-Hydroxyquinoline[a] (72–74)	119–121	1.15
7	Pyridine[b] (liquid)	143–145	0.008–0.030[c]
8	3-Hydroxy-6-methyl[b] (168–170)	162–164	0.005–0.020[c]
9	2-Amino[b] (59–60)	172–174	0.028–0.100[c]
10	3-Hydroxy[b] (126–129)	137–139	0.195–0.685[c]
11	2,2′-Bipyridyl[d] (70–73)		
12	2,6-Dibromo[d] (118–120)		
13	2,4,6-Trimethyl[d] (liquid)		
14	3-Carboxylic acid[d] (236–237)		
15	4-Carboxylic acid[d] (310–315, sub)		
16	2,5-Dicarboxylic acid[d] (256, dec)		
17	2-Cyano[d] (26–28)		

[a] Confirmed by satisfactory microanalyses. [b] Taken from ref. 17. [c] Data relative to quartz as given in ref. 17 have been converted relative to urea scale.[30] [d] Resisted salt formation with TA. [e] Not measured quantitatively.

Our previous efforts to design, synthesize and characterize 'push–pull' ethylenes and butadienes as NLO materials did not prove to be successful either due to the centrosymmetric nature of the crystals or unfavourable molecular packing.[8–12] Crystal engineering[13,14] is a powerful technique that allows one to elucidate relationships between molecular structure and lattice features in a predictable manner. But this is easier said than done because of the lack of adequate understanding of various intra- and inter-molecular interactions among the components which lead to the observed crystal packing. One of the most important and well understood interactions is hydrogen bonding.[15] Recently Aakeroy *et al.*[16–18] developed an elegant methodology to prepare novel classes of NLO active materials by using hydrogen bonding as the primary interaction. This procedure offers materials with favourable physical properties (*e.g.* absence of colour, solubility, thermal stability, needle like crystal morphology *etc.*) required for commercial applications. The methods of preparation did not involve difficult synthetic procedures also and offered scope for a wide variety of modifications. We are interested in understanding how the substituent variations in a given hetero-aromatic base affect the quantum of SHG intensities in the binary salts derived from individual bases with L-tartaric acid. Learning more about the solid state structural features may be important for designing future materials. Consequently, we have prepared a number of salts of L-tartaric acid (TA) and substituted pyridines. While we succeeded in preparing several salts, a number of pyridine derivatives persistently resisted salt formation (see below). In order to clearly understand the role of packing within a crystalline lattice of **1** towards the SHG activity, we have prepared single crystals of suitable quality for an X-ray diffraction experiment. A detailed X-ray crystal structure of one of the salts, *i.e.* L-tartaric acid–4-dimethylaminopyridine (1:1) dihydrate salt **1**, is presented in this paper. We have also quantitatively measured SHG activities of a number of salts that we have prepared. Finally, a rationale for the observed SHG activity has been provided based on the examination of packing modes in the crystalline assembly in **1**.

Results and Discussions

Table 1 records the physical characteristics of the salts prepared by us and compares some of the related salts reported by Aakeroy *et al.*[17] Single crystals from one representative salt **1** were grown and its X-ray structure was determined. Table 2 presents the selected bond lengths and angles of the non-hydrogen atoms. Hydrogen bonding parameters are given in

Table 2 Selected bond distances (Å) and bond angle (°) involving non hydrogen atoms of the L-tartaric acid–4-*N*,*N*-dimethylaminopyridine (1:1) dihydrate salt (esds in parentheses)

Bond	Distance	Bond	Distance
O(1)–C(1)	1.248(4)	C(3)–C(4)	1.540(5)
O(2)–C(1)	1.248(4)	C(5)–C(6)	1.421(6)
O(3)–C(2)	1.405(5)	C(5)–C(9)	1.422(7)
O(4)–C(3)	1.415(4)	C(5)–N(2)	1.338(5)
O(5)–C(4)	1.281(4)	C(6)–C(7)	1.337(8)
O(6)–C(4)	1.207(4)	C(7)–N(1)	1.340(8)
C(1)–C(2)	1.538(5)	C(8)–C(9)	1,342(8)
C(2)–C(3)	1.511(5)	C(8)–N(1)	1.343(10)
	Angle		
C(7)–N(1)–C(8)	120.3(5)		

Table 3 Hydrogen bonding parameters in **1**

D–H ··· A	H ··· A/Å	D ··· A/Å	D–H ··· A/°
O(4)–H(O4) ··· O(8)	1.949	2.766	137.2
O(5)–H(O5) ··· O(2)^a	1.621	2.497	161.8
O(3)^a–H(O3) ··· O(7)	1.858	2.803	169.0
O(8)^b–H(8A) ··· O(1)	1.945	2.730	157.1
O(8)^b–H(8B) ··· O(3)^a	2.227	2.864	159.7
O(7)^c–H(7A) ··· O(6)^a	2.016	2.732	168.1
N(1)^d–H(N1) ··· O(1)	2.268	2.996	127.5
O(7)^e–H(7B) ··· O(4)^a	2.087	2.784	169.1

Symmetry elements: ^{a} 1 + x, y, z; ^{b} −x, 0.5 + y, 0.5–z; ^{c} 1−x, y − 0.5, 0.5 − z; ^{d} −x, y − 0.5, 1.5 − z; ^{e} 2 − x, y − 0.5, 0.5 − z.

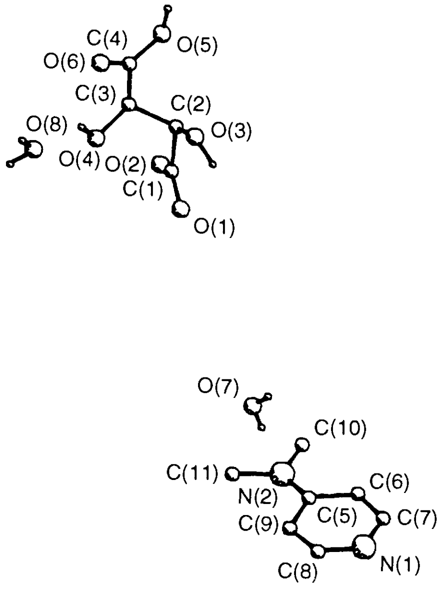

Fig. 1 Perspective view of **1** with atom numbering scheme

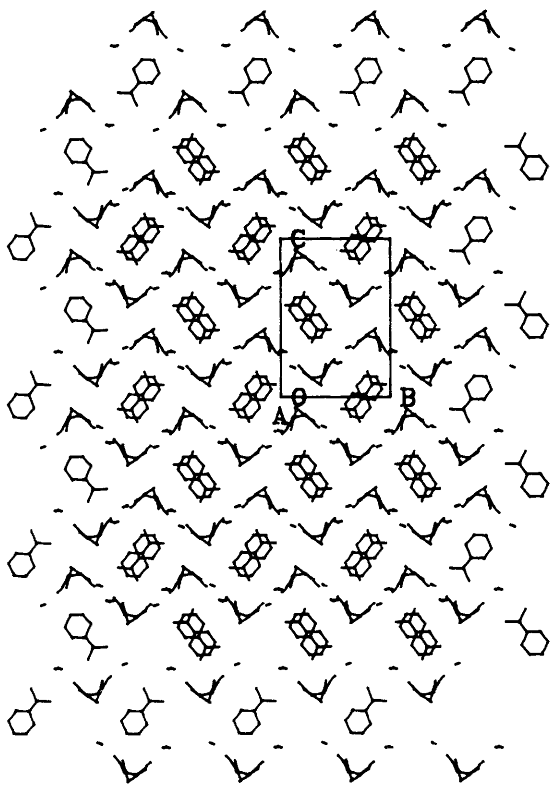

Fig. 2 Packing diagrams of the molecules of **1** viewed down shortest axis

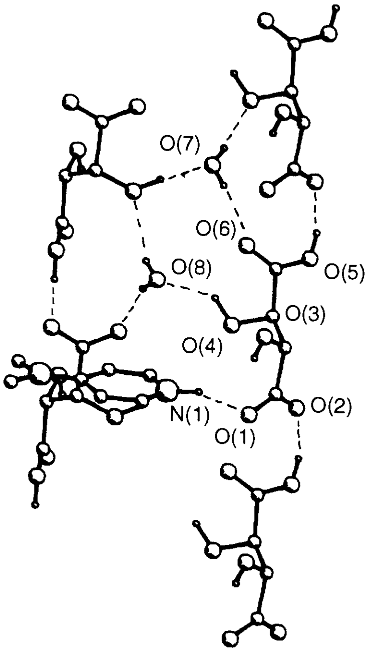

Fig. 3 Hydrogen bonding patterns in **1**

Table 3. Fig. 1 shows the molecular structure of **1** with its atomic numbering scheme. A packing diagram of **1** is shown in Fig. 2. Fig. 3 shows the hydrogen bonding patterns of **1**. Is there any correlation between the substituent variations in cations and the propensities to form hydrogen bond directed salts? In order to address this, we have concentrated our studies only on salts generated from pyridine and its derivatives. Interestingly, pyridines substituted with electron withdrawing groups (entries 14–17, Table 1) resisted binary salt formation. Electron-donating substituents, on the other hand, seem to favour salt formation with L-tartaric acid and the resulting salts are SHG active. Large *ortho* substituents *e.g.* that in 2,6-dibromopyridine prevented salt formation (entry 12, Table 1). However, all the salts that could be prepared are SHG active and their intensities fall in the range of that of urea and interestingly all of them show more pronounced SHG intensity relative to the ones already reported[17] for other pyridine derived TA salts (entries 7–10, Table 1). The position of the substituent on pyridine appears to be important also. Thus, 4-aminopyridinium L-tartrate is at least an order of magnitude more SHG active than its 2-amino substituted counterpart (entries 1 and 9, Table 1). It is interesting to note that water molecules of crystallization are present in all the salts except for the 4-(*p*-nitrobenzyl)pyridi-

nium salt on the basis of elemental analysis. The 4-(*p*-nitrobenzyl)pyridinium ion may be hydrophobic enough to resist water inclusion in the crystal lattice. It is clear from the Table 1 that there is no simple, apparent relationship between the nature of the substituents on pyridine and the intensities of the SHG activities observed. Obviously, it is not straightforward to compare the results obtained for different tartaric acid salts, because comparison can be made only between salts with similar crystal structures.

During our studies, we have found that L-tartaric acid is a SHG active material and its SHG intensity is comparable to that of urea. However, TA is soluble only in highly polar solvents and it is hygroscopic in nature and therefore it may not be a very useful material for incorporation into commercial devices. It is therefore justified to prepare salts of TA with organic bases which might provide more acceptable physical properties. It also offers abundant hydrogen bonding interactions to suitable bases. Thus, it is a very good starting material for the generation of salts with suitable bases. It is important to stress that these chiral anions are indispensable in these salts for SHG activity because they ensure a non-centrosymmetric feature in the resulting self-assembled crystalline lattice. However, the magnitude of SHG intensities do differ widely (compare entries 1–6 *vs.* 7–10, Table 1). Therefore, polarizable cations, although not chiral in nature, may play a crucial role in determining packing modes, hydrogen bonding motifs and L-tartrate conformation.

In the crystal structure of **1**, 4-dimethylaminopyridine (DMAP) takes up a proton through its ring nitrogen N(1) from TA. This is clear from the consideration of bond lengths and angles from the reported X-ray structure of free DMAP and its protonated analogue. In the crystal structure of free DMAP,[19] the bond distance of the exocyclic nitrogen to the ring carbon is found to be 1.367 Å. This is considerably reduced in 4-dimethylaminopyridinium hydrochloride dihydrate[20] (1.339 Å). Such reduction in bond distance of the exocyclic N to the ring carbon [C(5)–N(2) = 1.338(5) Å] in the DMAP moiety in **1** was also observed. This suggests that the delocalization of the unshared pair of electrons on exocyclic nitrogen is more pronounced in protonated DMAP than that in the non-protonated one. Manifestation of the effect of delocalization is also evident from the ring bond lengths. Considerable reduction in bond lengths in the aromatic ring [C(6)–C(7) = 1.337(8), C(8)–C(9) = 1.342(8) Å of DMAP in **1**, the corresponding lengths of DMAP in hydrochloride salt[20] are 1.346 and 1.348 Å respectively and these values are considerably shorter than the values of 1.375 and 1.381 Å in free DMAP[19]] suggests that the ring is in quinonoid form. According to a reported analysis,[21] the valence angle of the ring nitrogen atom in six membered heterocycles depends on the extraannular attachment of hydrogen to hetero N atom. In fact, the valence angle with an extraannular hydrogen attachment is 125.0 ± 0.2° whereas that without any attachment is 115.7 ± 0.2°. In free DMAP,[19] the valence angle is found to be 114.5° whereas the corresponding values are 119.8° and 120.3(5)° in DMAP hydrochloride[20] and in DMAP in **1** respectively. These values are in agreement with the analyses and once again indicate that DMAP in **1** is protonated *via* the ring nitrogen.

An extensive hydrogen bonding network is observed in this structure. TA is in its monoanionic form ($-CO_2H$, COO^-) and it forms an infinite chain of TA along the *a*-axis through $COO^- \cdots HO_2C$ type of hydrogen bonding [O(2) ··· O(5) = 2.497 Å] network. There are two solvent water molecules in the crystal lattice. Both the solvent molecules act as bridges between two infinite chains of TA through hydrogen bonding (Fig. 3). Each one holds three symmetry related TA molecules [O(8) ··· O(4) = 2.766, O(8) ··· O(1) = 2.730, O(8) ··· O(3) = 2.864 Å; O(7) ··· O(3) = 2.803, O(7) ··· O(6) = 2.732, O(7) ··· O(4) = 2.784 Å]. DMAP holds one TA molecule through the hydrogen attached to ring nitrogen [N(1) ··· O(1) = 2.996 Å].

We also detected the presence of C–H ··· O type hydrogen bonding where one solvent water molecule is held by a methylamino group [C(10) ··· O(8) = 3.229; O(8) ··· H-(10C) = 2.413 Å; C(10)–H(10C) ··· O(8) = 139.4°]. Crystallographic evidence for the existence of C–H ··· O type hydrogen bonding was provided first by Taylor *et al.*[22] Database analyses suggested that C–H groups that are adjacent to nitrogen atoms are likely to participate in this type of hydrogen bonding.[22] In order to understand complex hydrogen bonding patterns, Etter *et al.*[23] developed a method based on graph set theory. This method decodes, systematically and consistently, the complex hydrogen bonding patterns. A graph set is specified using the pattern designator (*G*), its degree (*r*) and the number of donors (*d*) and acceptors (*a*) as $G^a_d(r)$. *G*, the hydrogen bond pattern descriptor, can be either S(intramolecular), C(infinite chain), R(ring) or D(non cyclic dimer or other finite hydrogen bonded set). The parameter *r* refers to the degree, being either the number of atoms in a ring or the repeat length of a chain. The set of molecules to be analysed is called an array. Graph sets are assigned initially to motifs (hydrogen bonded set constructed by only one type of hydrogen bond) and then to first level network (a combination of all the relevant motifs *e.g.* if the array contains seven motifs, then the first level network is a combination of seven motifs). Based on this analysis, we have assigned the first order network to **1** as $N_1 = 4DC^1_1(7)$. This represents the hydrogen bonding pattern in a simple way; an infinite chain of repeat units seven and four dimeric hydrogen bonds are present. Three of them are O–H ··· O type and the other one is N–H ··· O type.

SHG Intensity and Molecular Packing Correlation.—The packing diagram (Fig. 2) shows that the cations, 4-dimethylaminopyridinum, are exactly oppositely oriented to each other and therefore the contribution of the dipoles from the cations to the macroscopic second-order susceptibility X^2 is zero. As the material is SHG active, this has to come from the dipole contribution from the TA anion. Thus, we have calculated the ground state dipole moment of TA anion using the same conformation as is found in this crystal structure of **1** by the AM1[24] method and it is found to be 10.294 D. According to Zyss and Oudar,[7] the charge transfer axis (CT) should make an angle of 54.74° with the crystallographic *b*-axis in order to produce maximum nonlinear response for the point group 222. In the present case, the resultant dipole moment vector *i.e.* CT axis of TA anion makes angles 61.3°, 47.9° and 55.9° with *a*, *b* and *c* axes respectively. The value of 47.9° is not far away from the calculated optimum value of 54.74°. Allowing the Kleinman symmetry,[25] three non-vanishing nonlinear coefficients[26] for this point group 222 become a single component *d*. This is given by the relation (1); where *N* is the number of molecules per unit

$$d = 4Nf^3 \cos(X, a) \cos(X, b) \cos(X, c)\beta \qquad (1)$$

volume and *f* is a local field factor at frequency *w* which determines the value of electric field at the site of the molecule. If any one of the cosine projection factors cancel out, *d* becomes zero. In the present study, the charge transfer axis does not make any angle which leads to the cosine projection factor equal to zero and therefore this material shows SHG intensity as high as urea even though the contributions from the cations are zero.

It is clear from the above discussion that analyses of packing arrangements within the crystal lattice of **1** allows us to interpret the SHG activity of this salt. It may be possible that the conclusion drawn in this study may well be applied to any salt derived from 4-aminopyridine. However, the generality of such conclusions may not be valid for salts that contain cations with markedly different substitution patterns. By systematic structural variation of the molecular achitecture and crystal engineering, we are currently applying similar strategies in related classes of molecular materials in order to gain a prediction about the SHG activity.

Experimental

Salts were prepared by dissolving a 1 : 1 molar mixture of L-tartaric acid and the corresponding pyridine derivatives in a methanol–water mixture. SHGs of the salts were measured by using a powder technique.[27] Crystals of **1** were grown by a slow evaporation technique at room temp. from 1 : 1 methanol–water solution.

*Crystal Data.**—**1**: $[C_4H_5O_6]^{1-}$ $[C_7H_{11}N_2]^{1+}\cdot 2H_2O$, M = 308.2, orthorhombic, a = 7.321(1), b = 11.846(1), c = 16.469(1) Å, V = 1428.2(2) Å^3 (by least-squares refinement on diffractometer angles for 25 automatically centred reflections in the range $15° \geqslant \theta \geqslant 6°$, MoKα radiation, = 0.7107 Å, space group $P2_12_12_1$, z = 4, D_{calc} = 1.433 g cm^{-3}, colourless needle. Crystal dimensions 0.15 × 0.15 × 0.5 mm, μ = 1.149 cm^{-1}.

Data collection and processing. Data were collected on an Enraf Nonius CAD-4 diffractometer in $\omega/2\theta$ scan mode with a pre-scan speed of 5.5° min^{-1} and the final scan was done with a scan speed calculated to satisfy the condition $\sigma(I)/I \leqslant 0.03$. 1245 Reflections measured ($0 \leqslant 2\theta \leqslant 46.94$; index range $0 \leqslant h \leqslant 8$, $0 \leqslant k \leqslant 13$, $0 \leqslant l \leqslant 18$), 1234 unique reflections of which 1146 ($I > 3\sigma(I)$) are significant. Three standard reflections (142, 116, 132) after every 3600 s of data collection were used to monitor the stability of the crystal. Orientation was checked after every 400 reflections. However, no significant fluctuations in the orientation or intensities were observed. The data were corrected for Lorentz and polarization effects, but not for extinction and absorption effects.

Structure solution and refinement. The structure solution of **1** was not straightforward. A direct method run using SHELXS66 program[28] did not give the full structure. Only a small fragment with meaningful contacts appeared on the E-map. Subsequent phase expansions using this fragment as a starting model eventually gave all non-hydrogen atoms. The refinement was carried out by a full matrix least-squares program SHELX76.[29] The parameters for non-hydrogen atoms were refined anisotropically. All the hydrogen atoms except those attached to methyl groups of DMAP were located on a difference Fourier map. Hydrogens attached to the methyl groups are at their stereochemically calculated positions. The positional and isotropic thermal parameters of five hydrogen atoms namely H(2), H(3), H(6), H(8) and H(9) were refined but the other hydrogen parameters were kept fixed. However, their contributions to structure factor calculations were considered at the final cycles of refinement. The final cycle of refinement on $|F|$ included 211 variables and converged to R = 0.047, wR = 0.055 and S = 0.98. Weighting scheme defined as $w = k/\sigma^2(F) + gF^2$ where k = 1.0 and g = 0.004836, function minimized was $\Sigma w(|F_0| - |F_C|)^2$, $(\Delta/\sigma)_{\max}$ 0.013, final difference Fourier syntheses: $-0.172 \leqslant \Delta\rho \leqslant 0.001$ e Å^{-3}. Atomic scattering factors as supplied with SHELX76.

Acknowledgements

We thank Professor C. N. R. Rao, Director, Indian Institute of Science and STC, ISRO for financial support, Professor K. Venkatesan for useful discussions and Ms. Renuka K. for assistance. One of us (P. D.) acknowledges UGC, India for senior research fellowship. We also thank one of the referees for raising pertinent points about the manuscript.

References

1 P. N. Prasad and D. J. Williams, *Introduction to Nonlinear Optical Effects in Molecules and Polymers*, Wiley, New York, 1990.

2 D. Williams, in *Electronic and Photonic Applications of Polymers*, eds. M. J. Bowden and S. R. Turner, American Chemical Society, Washington D.C. 1988, 218th edn.

3 (*a*) R. G. Hunsperger, in *Integrated Optics: Theory and Technology*, 2nd edn., Springer-Verlag, New York, 1984, p. 127; (*b*) D. R. Ulrich, *Mol. Cryst. Liq. Cryst.*, 1990, **189**, 3.

4 D. M. Pepper, *Sci. Am.*, 1986, **254**, 74.

5 *Nonlinear Optical Properties of Organic Molecules and Crystals*, eds. D. S. Chemla and J. Zyss, Academic Press, New York, 1987, vols. 1 and 2.

6 *Materials for Nonlinear Optics*, eds. S. R. Marder, J. E. Sohn and G. D. Stucky, ACS Symp. Ser. 455, American Chemical Society, Washington D.C., 1991.

7 J. Zyss and J. L. Oudar, *Phys. Rev.*, 1982, **A26**, 2028.

8 D. Kanagapushpam and K. Venkatesan, *Acta Crystallogr., Sect. C, Cryst. Struct. Commun.*, 1987, **43**, 1597.

9 D. Kanagapushpam, K. Padmanabhan and K. Venkatesan, *Acta Crystallogr., Sect. C, Cryst. Struct. Commun.*, 1987, **43**, 1717.

10 D. Kanagapushpam, K. Venkatesan and T. S. Cameron, *Acta Crystallogr, Sect. C, Cryst. Struct. Commun.*, 1988, **44**, 337.

11 P. Dastidar, T. N. Guru Row and K. Venkatesan, *J. Mater. Chem.*, 1991, **1**, 1057.

12 P. Dastidar, T. N. Guru Row and K. Venkatesan, *Acta Crystallogr. Sect. B., Struct. Sci.*, 1993, in the press.

13 G. R. Desiraju, in *Crystal Engineering. The Design of Organic Solids*, Elsevier, Amsterdam, 1989.

14 J.-M. Lehn, *Angew. Chem., Int. Ed. Engl.*, 1990, **29**, 1304.

15 *The Hydrogen Bond*, eds. D. Schuster, G. Zundel and C. Zandorfy, North-Holland, Amsterdam, 1976, vols. 1–111.

16 C. B. Aakeroy, P. B. Hitchcock, B. D. Moyle and K. R. Seddon, *J. Chem. Soc., Chem. Commun.*, 1989, 1856.

17 C. B. Aakeroy, P. B. Hitchcock, K. R. Seddon, *J. Chem. Soc., Chem. Commun.*, 1992, 553.

18 C. B. Aakeroy, G. S. Bahra, P. B. Hitchcock, Y. Patell and K. R. Seddon, *J. Chem. Soc., Chem. Commun.*, 1993, 152.

19 U. Ohms and H. Guth, *Z. Kristallogr.*, 1984, **166**, 213.

20 H. Chao, E. Schempp and R. D. Rosenstein, *Acta Crystallogr. Sect. B., Struct. Crystallogr.* 1977, **38**, 1820.

21 C. Singh, *Acta Crystallogr.*, 1965, **19**, 861.

22 R. Taylor and O. Kennard, *J. Am. Chem. Soc.*, 1982, **104**, 5063.

23 M. C. Etter and J. C. MacDonald, *Acta Crystallogr. Sect. B, Struct. Sci.*, 1990, **46**, 256.

24 M. J. S. Dewar, E. G. Zoebisch, E. F. Healy and J. J. P. Stewart, *J. Am. Chem. Soc.*, 1985, **107**, 3902.

25 D. A. Kleinman, *Phys. Rev.*, 1962, **126**, 1977.

26 P. N. Butcher, in *Nonlinear Optical Phenomena*, Ohio State University, Columbus, Ohio, 1965.

27 S. K. Kurtz and T. T. Perry, *J. Appl. Phys.*, 1968, **39**, 3798.

28 G. M. Sheldrick, SHELXS86, program for crystal structure solution, Gottingen University, Germany.

29 G. M. Sheldrick, SHELX76, program for crystal structure determination, University of Cambridge, UK.

30 J. F. Nicoud and R. J. Twieg, in *Nonlinear Optical Properties of Organic Molecules and Crystals*, ed. D. S. Chemla and J. Zyss, Academic Press, New York, 1987, vol. 2.

Paper 3/02752J
Received 14*th May* 1993
Accepted 11*th August* 1993

---

* Crystallographic Data has been deposited at the Cambridge Crystallographic Data Centre. For details of the deposition scheme, see 'Instructions for Authors', *J. Chem. Soc.*, Perkin Trans. 2, 1993, issue 1.